

Measurement of the Inclusive Electron Spectrum in Charmless Semileptonic B Decays Near the Kinematic Endpoint

The *BABAR* Collaboration

July 24, 2002

Abstract

A preliminary result on the study of the inclusive electron spectrum in $B \rightarrow X_u e \nu$ decays above the kinematic limit for the dominant $B \rightarrow X_c e \nu$ transitions is presented. This study is performed at the PEP-II asymmetric B Factory, where B meson pairs are produced in the decay of the $\Upsilon(4S)$ resonance. For the electron momentum range of $2.3 - 2.6$ GeV/ c in the $\Upsilon(4S)$ rest frame, the partial branching ratio is measured to be $\Delta\mathcal{B}(B \rightarrow X_u e \nu) = (0.152 \pm 0.014 \pm 0.014) \cdot 10^{-3}$.

Contributed to the 31st International Conference on High Energy Physics,
7/24—7/31/2002, Amsterdam, The Netherlands

Stanford Linear Accelerator Center, Stanford University, Stanford, CA 94309

Work supported in part by Department of Energy contract DE-AC03-76SF00515.

The BABAR Collaboration,

B. Aubert, D. Boutigny, J.-M. Gaillard, A. Hicheur, Y. Karyotakis, J. P. Lees, P. Robbe, V. Tisserand,
A. Zghiche

Laboratoire de Physique des Particules, F-74941 Annecy-le-Vieux, France

A. Palano, A. Pompili

Università di Bari, Dipartimento di Fisica and INFN, I-70126 Bari, Italy

J. C. Chen, N. D. Qi, G. Rong, P. Wang, Y. S. Zhu

Institute of High Energy Physics, Beijing 100039, China

G. Eigen, I. Ofte, B. Stugu

University of Bergen, Inst. of Physics, N-5007 Bergen, Norway

G. S. Abrams, A. W. Borgland, A. B. Breon, D. N. Brown, J. Button-Shafer, R. N. Cahn, E. Charles,
M. S. Gill, A. V. Gritsan, Y. Groysman, R. G. Jacobsen, R. W. Kadel, J. Kadyk, L. T. Kerth,
Yu. G. Kolomensky, J. F. Kral, C. LeClerc, M. E. Levi, G. Lynch, L. M. Mir, P. J. Oddone, T. J. Orimoto,
M. Pripstein, N. A. Roe, A. Romosan, M. T. Ronan, V. G. Shelkov, A. V. Telnov, W. A. Wenzel

Lawrence Berkeley National Laboratory and University of California, Berkeley, CA 94720, USA

T. J. Harrison, C. M. Hawkes, D. J. Knowles, S. W. O'Neale, R. C. Penny, A. T. Watson, N. K. Watson

University of Birmingham, Birmingham, B15 2TT, United Kingdom

T. Deppermann, K. Goetzen, H. Koch, B. Lewandowski, K. Peters, H. Schmuecker, M. Steinke

Ruhr Universität Bochum, Institut für Experimentalphysik 1, D-44780 Bochum, Germany

N. R. Barlow, W. Bhimji, J. T. Boyd, N. Chevalier, P. J. Clark, W. N. Cottingham, C. Mackay,
F. F. Wilson

University of Bristol, Bristol BS8 1TL, United Kingdom

K. Abe, C. Hearty, T. S. Mattison, J. A. McKenna, D. Thiessen

University of British Columbia, Vancouver, BC, Canada V6T 1Z1

S. Jolly, A. K. McKemey

Brunel University, Uxbridge, Middlesex UB8 3PH, United Kingdom

V. E. Blinov, A. D. Bukin, A. R. Buzykaev, V. B. Golubev, V. N. Ivanchenko, A. A. Korol,
E. A. Kravchenko, A. P. Onuchin, S. I. Serebnyakov, Yu. I. Skovpen, A. N. Yushkov

Budker Institute of Nuclear Physics, Novosibirsk 630090, Russia

D. Best, M. Chao, D. Kirkby, A. J. Lankford, M. Mandelkern, S. McMahon, D. P. Stoker

University of California at Irvine, Irvine, CA 92697, USA

C. Buchanan, S. Chun

University of California at Los Angeles, Los Angeles, CA 90024, USA

H. K. Hadavand, E. J. Hill, D. B. MacFarlane, H. Paar, S. Prell, Sh. Rahatlou, G. Raven, U. Schwanke,
V. Sharma

University of California at San Diego, La Jolla, CA 92093, USA

J. W. Berryhill, C. Campagnari, B. Dahmes, P. A. Hart, N. Kuznetsova, S. L. Levy, O. Long, A. Lu,
M. A. Mazur, J. D. Richman, W. Verkerke

University of California at Santa Barbara, Santa Barbara, CA 93106, USA

J. Beringer, A. M. Eisner, M. Grothe, C. A. Heusch, W. S. Lockman, T. Pulliam, T. Schalk, R. E. Schmitz,
B. A. Schumm, A. Seiden, M. Turri, W. Walkowiak, D. C. Williams, M. G. Wilson

University of California at Santa Cruz, Institute for Particle Physics, Santa Cruz, CA 95064, USA

E. Chen, G. P. Dubois-Felsmann, A. Dvoretzki, D. G. Hitlin, F. C. Porter, A. Ryd, A. Samuel, S. Yang
California Institute of Technology, Pasadena, CA 91125, USA

S. Jayatileke, G. Mancinelli, B. T. Meadows, M. D. Sokoloff

University of Cincinnati, Cincinnati, OH 45221, USA

T. Barillari, P. Bloom, W. T. Ford, U. Nauenberg, A. Olivas, P. Rankin, J. Roy, J. G. Smith, W. C. van
Hoek, L. Zhang

University of Colorado, Boulder, CO 80309, USA

J. L. Harton, T. Hu, M. Krishnamurthy, A. Soffer, W. H. Toki, R. J. Wilson, J. Zhang

Colorado State University, Fort Collins, CO 80523, USA

D. Altenburg, T. Brandt, J. Brose, T. Colberg, M. Dickopp, R. S. Dubitzky, A. Hauke, E. Maly,
R. Müller-Pfefferkorn, S. Otto, K. R. Schubert, R. Schwierz, B. Spaan, L. Wilden

Technische Universität Dresden, Institut für Kern- und Teilchenphysik, D-01062 Dresden, Germany

D. Bernard, G. R. Bonneaud, F. Brochard, J. Cohen-Tanugi, S. Ferrag, S. T'Jampens, Ch. Thiebaux,
G. Vasileiadis, M. Verderi

Ecole Polytechnique, LLR, F-91128 Palaiseau, France

A. Anjomshoa, R. Bernet, A. Khan, D. Lavin, F. Muheim, S. Playfer, J. E. Swain, J. Tinslay

University of Edinburgh, Edinburgh EH9 3JZ, United Kingdom

M. Falbo

Elon University, Elon University, NC 27244-2010, USA

C. Borean, C. Bozzi, L. Piemontese, A. Sarti

Università di Ferrara, Dipartimento di Fisica and INFN, I-44100 Ferrara, Italy

E. Treadwell

Florida A&M University, Tallahassee, FL 32307, USA

F. Anulli,¹ R. Baldini-Ferrolì, A. Calcaterra, R. de Sangro, D. Falciai, G. Finocchiaro, P. Patteri,
I. M. Peruzzi,¹ M. Piccolo, A. Zallo

Laboratori Nazionali di Frascati dell'INFN, I-00044 Frascati, Italy

S. Bagnasco, A. Buzzo, R. Contri, G. Crosetti, M. Lo Vetere, M. Macri, M. R. Monge, S. Passaggio,
F. C. Pastore, C. Patrignani, E. Robutti, A. Santroni, S. Tosi

Università di Genova, Dipartimento di Fisica and INFN, I-16146 Genova, Italy

¹Also with Università di Perugia, I-06100 Perugia, Italy

S. Bailey, M. Morii

Harvard University, Cambridge, MA 02138, USA

R. Bartoldus, G. J. Grenier, U. Mallik

University of Iowa, Iowa City, IA 52242, USA

J. Cochran, H. B. Crawley, J. Lamsa, W. T. Meyer, E. I. Rosenberg, J. Yi

Iowa State University, Ames, IA 50011-3160, USA

M. Davier, G. Grosdidier, A. Höcker, H. M. Lacker, S. Laplace, F. Le Diberder, V. Lepeltier, A. M. Lutz,
T. C. Petersen, S. Plaszczynski, M. H. Schune, L. Tantot, S. Trincaz-Duvoid, G. Wormser

Laboratoire de l'Accélérateur Linéaire, F-91898 Orsay, France

R. M. Bionta, V. Brigljević, D. J. Lange, K. van Bibber, D. M. Wright

Lawrence Livermore National Laboratory, Livermore, CA 94550, USA

A. J. Bevan, J. R. Fry, E. Gabathuler, R. Gamet, M. George, M. Kay, D. J. Payne, R. J. Sloane,
C. Touramanis

University of Liverpool, Liverpool L69 3BX, United Kingdom

M. L. Aspinwall, D. A. Bowerman, P. D. Dauncey, U. Egede, I. Eschrich, G. W. Morton, J. A. Nash,
P. Sanders, D. Smith, G. P. Taylor

University of London, Imperial College, London, SW7 2BW, United Kingdom

J. J. Back, G. Bellodi, P. Dixon, P. F. Harrison, R. J. L. Potter, H. W. Shorthouse, P. Strother, P. B. Vidal

Queen Mary, University of London, E1 4NS, United Kingdom

G. Cowan, H. U. Flaecher, S. George, M. G. Green, A. Kurup, C. E. Marker, T. R. McMahon, S. Ricciardi,
F. Salvatore, G. Vaitsas, M. A. Winter

University of London, Royal Holloway and Bedford New College, Egham, Surrey TW20 0EX, United Kingdom

D. Brown, C. L. Davis

University of Louisville, Louisville, KY 40292, USA

J. Allison, R. J. Barlow, A. C. Forti, F. Jackson, G. D. Lafferty, A. J. Lyon, N. Savvas, J. H. Weatherall,
J. C. Williams

University of Manchester, Manchester M13 9PL, United Kingdom

A. Farbin, A. Jawahery, V. Lillard, D. A. Roberts, J. R. Schieck

University of Maryland, College Park, MD 20742, USA

G. Blaylock, C. Dallapiccola, K. T. Flood, S. S. Hertzbach, R. Kofler, V. B. Koptchey, T. B. Moore,
H. Staengle, S. Willocq

University of Massachusetts, Amherst, MA 01003, USA

B. Brau, R. Cowan, G. Sciolla, F. Taylor, R. K. Yamamoto

Massachusetts Institute of Technology, Laboratory for Nuclear Science, Cambridge, MA 02139, USA

M. Milek, P. M. Patel

McGill University, Montréal, QC, Canada H3A 2T8

F. Palombo

Università di Milano, Dipartimento di Fisica and INFN, I-20133 Milano, Italy

J. M. Bauer, L. Cremaldi, V. Eschenburg, R. Kroeger, J. Reidy, D. A. Sanders, D. J. Summers
University of Mississippi, University, MS 38677, USA

C. Hast, P. Taras

Université de Montréal, Laboratoire René J. A. Lévesque, Montréal, QC, Canada H3C 3J7

H. Nicholson

Mount Holyoke College, South Hadley, MA 01075, USA

C. Cartaro, N. Cavallo, G. De Nardo, F. Fabozzi, C. Gatto, L. Lista, P. Paolucci, D. Piccolo, C. Sciacca
Università di Napoli Federico II, Dipartimento di Scienze Fisiche and INFN, I-80126, Napoli, Italy

J. M. LoSecco

University of Notre Dame, Notre Dame, IN 46556, USA

J. R. G. Alsmiller, T. A. Gabriel

Oak Ridge National Laboratory, Oak Ridge, TN 37831, USA

J. Brau, R. Frey, M. Iwasaki, C. T. Potter, N. B. Sinev, D. Strom, E. Torrence

University of Oregon, Eugene, OR 97403, USA

F. Colecchia, A. Dorigo, F. Galeazzi, M. Margoni, M. Morandin, M. Posocco, M. Rotondo, F. Simonetto,
R. Stroili, C. Voci

Università di Padova, Dipartimento di Fisica and INFN, I-35131 Padova, Italy

M. Benayoun, H. Briand, J. Chauveau, P. David, Ch. de la Vaissière, L. Del Buono, O. Hamon,
Ph. Leruste, J. Ocariz, M. Pivk, L. Roos, J. Stark

Universités Paris VI et VII, Lab de Physique Nucléaire H. E., F-75252 Paris, France

P. F. Manfredi, V. Re, V. Speziali

Università di Pavia, Dipartimento di Elettronica and INFN, I-27100 Pavia, Italy

L. Gladney, Q. H. Guo, J. Panetta

University of Pennsylvania, Philadelphia, PA 19104, USA

C. Angelini, G. Batignani, S. Bettarini, M. Bondioli, F. Bucci, G. Calderini, E. Campagna, M. Carpinelli,
F. Forti, M. A. Giorgi, A. Lusiani, G. Marchiori, F. Martinez-Vidal, M. Morganti, N. Neri, E. Paoloni,
M. Rama, G. Rizzo, F. Sandrelli, G. Triggiani, J. Walsh

Università di Pisa, Scuola Normale Superiore and INFN, I-56010 Pisa, Italy

M. Haire, D. Judd, K. Paick, L. Turnbull, D. E. Wagoner

Prairie View A&M University, Prairie View, TX 77446, USA

J. Albert, G. Cavoto,² N. Danielson, P. Elmer, C. Lu, V. Miftakov, J. Olsen, S. F. Schaffner,
A. J. S. Smith, A. Tumanov, E. W. Varnes

Princeton University, Princeton, NJ 08544, USA

²Also with Università di Roma La Sapienza, Roma, Italy

F. Bellini, D. del Re, R. Faccini,³ F. Ferrarotto, F. Ferroni, E. Leonardi, M. A. Mazzone, S. Morganti,
G. Piredda, F. Safai Tehrani, M. Serra, C. Voena

Università di Roma La Sapienza, Dipartimento di Fisica and INFN, I-00185 Roma, Italy

S. Christ, G. Wagner, R. Waldi

Universität Rostock, D-18051 Rostock, Germany

T. Adye, N. De Groot, B. Franek, N. I. Geddes, G. P. Gopal, S. M. Xella

Rutherford Appleton Laboratory, Chilton, Didcot, Oxon, OX11 0QX, United Kingdom

R. Aleksan, S. Emery, A. Gaidot, P.-F. Giraud, G. Hamel de Monchenault, W. Kozanecki, M. Langer,
G. W. London, B. Mayer, G. Schott, B. Serfass, G. Vasseur, Ch. Yeche, M. Zito

DAPNIA, Commissariat à l'Energie Atomique/Saclay, F-91191 Gif-sur-Yvette, France

M. V. Purohit, A. W. Weidemann, F. X. Yumiceva

University of South Carolina, Columbia, SC 29208, USA

I. Adam, D. Aston, N. Berger, A. M. Boyarski, M. R. Convery, D. P. Coupal, D. Dong, J. Dorfan,
W. Dunwoodie, R. C. Field, T. Glanzman, S. J. Gowdy, E. Grauges, T. Haas, T. Hadig, V. Halyo,
T. Himel, T. Hryn'ova, M. E. Huffer, W. R. Innes, C. P. Jessop, M. H. Kelsey, P. Kim, M. L. Kocian,
U. Langenegger, D. W. G. S. Leith, S. Luitz, V. Luth, H. L. Lynch, H. Marsiske, S. Menke, R. Messner,
D. R. Muller, C. P. O'Grady, V. E. Ozcan, A. Perazzo, M. Perl, S. Petrak, H. Quinn, B. N. Ratcliff,
S. H. Robertson, A. Roodman, A. A. Salnikov, T. Schietinger, R. H. Schindler, J. Schwiening, G. Simi,
A. Snyder, A. Soha, S. M. Spanier, J. Stelzer, D. Su, M. K. Sullivan, H. A. Tanaka, J. Va'vra,
S. R. Wagner, M. Weaver, A. J. R. Weinstein, W. J. Wisniewski, D. H. Wright, C. C. Young

Stanford Linear Accelerator Center, Stanford, CA 94309, USA

P. R. Burchat, C. H. Cheng, T. I. Meyer, C. Roat

Stanford University, Stanford, CA 94305-4060, USA

R. Henderson

TRIUMF, Vancouver, BC, Canada V6T 2A3

W. Bugg, H. Cohn

University of Tennessee, Knoxville, TN 37996, USA

J. M. Izen, I. Kitayama, X. C. Lou

University of Texas at Dallas, Richardson, TX 75083, USA

F. Bianchi, M. Bona, D. Gamba

Università di Torino, Dipartimento di Fisica Sperimentale and INFN, I-10125 Torino, Italy

L. Bosisio, G. Della Ricca, S. Dittongo, L. Lanceri, P. Poropat, L. Vitale, G. Vuagnin

Università di Trieste, Dipartimento di Fisica and INFN, I-34127 Trieste, Italy

R. S. Panvini

Vanderbilt University, Nashville, TN 37235, USA

³Also with University of California at San Diego, La Jolla, CA 92093, USA

S. W. Banerjee, C. M. Brown, D. Fortin, P. D. Jackson, R. Kowalewski, J. M. Roney

University of Victoria, Victoria, BC, Canada V8W 3P6

H. R. Band, S. Dasu, M. Datta, A. M. Eichenbaum, H. Hu, J. R. Johnson, R. Liu, F. Di Lodovico,
A. Mohapatra, Y. Pan, R. Prepost, I. J. Scott, S. J. Sekula, J. H. von Wimmersperg-Toeller, J. Wu,
S. L. Wu, Z. Yu

University of Wisconsin, Madison, WI 53706, USA

H. Neal

Yale University, New Haven, CT 06511, USA

1 Introduction

The principal physics goal of the *BABAR* experiment is to establish CP -violation in B mesons and to test whether the observed effects are consistent with the prediction of the Standard Model. In this model CP violating effects are predicted from the CKM matrix of the couplings of the charged weak current to quarks. A precise determination of the matrix element $|V_{ub}|$ will place constraints on the unitarity of the CKM matrix and thus the consistency with the minimal Standard Model.

The extraction of $|V_{ub}|$ is a challenge, both theoretically and experimentally. While at the parton level weak interactions can be reliably calculated, meson decays depend on the b quark mass and its motion inside the B meson. Theoretical calculations of the semileptonic decay rate in terms of $|V_{ub}|$ rely on an operator product expansion (OPE) in inverse powers of the b quark mass [1] and thus depend on the choice of renormalization scale and include non-perturbative parameters. Experimentally, the principal difficulty is the separation of $B \rightarrow X_u e \nu$ decays from the dominant $B \rightarrow X_c e \nu$ decays. Selection criteria applied to achieve this separation generally make it difficult to translate the observed rate to the full decay rate.

In this paper we present a measurement of the inclusive electron spectrum for charmless semileptonic B decays in the momentum range of $2.3 - 2.6$ GeV/ c as measured in the $\Upsilon(4S)$ rest frame. In the rest frame of the B meson, the kinematic endpoint of the electron spectrum for the dominant $B \rightarrow X_c e \nu$ decays is ~ 2.3 GeV/ c and ~ 2.6 GeV/ c for $B \rightarrow X_u e \nu$ decays. In the rest frame of the $\Upsilon(4S)$, the B mesons have a momentum of ~ 0.3 GeV/ c and thus the electron spectrum is convoluted by a spread of ± 0.2 GeV/ c , extending the endpoint to higher energies. Nevertheless, a narrow interval of about 300 MeV/ c remains that is dominated by electrons from $B \rightarrow X_u e \nu$ transitions. This interval covers approximately 10% of the total electron spectrum for charmless semileptonic B decays. The extrapolation from the limited momentum range near the endpoint to the full spectrum is a very difficult task because the OPE breaks down in this part of phase space.

This analysis is based on the same method as previous measurements of the lepton spectrum near the endpoint [2, 3] (ARGUS), [4, 5] (CLEO).

2 Detector and Data Sample

This analysis is based on data recorded in 1999-2000 with the *BABAR* detector at the PEP-II energy asymmetric e^+e^- collider at the Stanford Linear Accelerator Center. The data sample corresponds to an integrated luminosity of 20.6 fb^{-1} that was collected at the $\Upsilon(4S)$ resonance (ON), plus an additional sample of 2.6 fb^{-1} that was recorded about 40 MeV below the $\Upsilon(4S)$ peak (OFF).

The relative normalization of the ON and OFF-peak data is $7.87 \pm 0.01 \pm 0.04$. This factor has been derived from luminosity measurements, which are based on the QED cross section for $e^+e^- \rightarrow \mu^+\mu^-$ production, corrected for the energy dependence of the cross section. The systematic error on the relative normalization is estimated to be $\sim 0.5\%$. This error accounts for small variations in the detector response and is significantly smaller than the systematic error of $\sim 1.6\%$ on the absolute $\mu^+\mu^-$ cross section measurement.

The *BABAR* detector has been described in detail elsewhere [6]. The most important components for this study are the charged particle tracking system, consisting of a five-layer silicon detector and a 40-layer drift chamber, and the electromagnetic calorimeter assembled from 6580 CsI(Tl) crystals. Electron candidates are selected on the basis of the ratio of the energy detected in the calorimeter to the track momentum, the calorimeter shower shape, the energy loss in the drift chamber, and the angle reconstructed in the ring imaging Cherenkov detector.

The electron identification efficiency and the probabilities to misidentify a pion, kaon, or proton as an electron have been measured with clean samples of tracks that were selected from the data. This experimental information is introduced into the Monte Carlo simulation to improve the agreement with the data. Tracking efficiencies and resolution have been studied. A comparison with the simulation has revealed small differences, which have been taken into account. No significant impact of non-Gaussian resolution tails has been found in the endpoint region.

The Monte Carlo simulation of $B \rightarrow X_u e \nu$ events is based on the ISGW2 model [7]. In the current version, the hadrons X_u are represented by single particles or resonances with masses up to 1.5 GeV/ c^2 and non-resonant contributions are not included. For $B \rightarrow X_c e \nu$ transitions three models are employed to simulate different decay modes. The decay to $D^* e \nu$ is modeled following a form factor based parameterization of HQET [8]; for decays to $D e \nu$ and higher mass charm meson states the ISGW2 model is used. The non-resonant decays to $D^{(*)} \pi e \nu$ are modeled according to a prescription by Goity and Roberts [9].

3 Data Analysis

3.1 Event Selection

For this analysis, electron candidates are selected in the momentum range from 1.5 to 3.5 GeV/ c in the $\mathcal{Y}(4S)$ rest frame. The solid angle is restricted by the electromagnetic calorimeter coverage, defined by the laboratory polar angle range of $-0.72 < \cos \theta_{\text{lab}} < 0.92$. In this momentum and angular range, the efficiency for identifying an electron has been measured to be $\epsilon_{PID} = 0.91 \pm 0.02$, while the average hadron misidentification probability is less than 0.2%. The selected electron sample is dominated by electrons from semileptonic decays of B and D mesons, non-resonant $q\bar{q}$ production and QED processes. In addition, photon conversions and Dalitz decays contribute background at low momenta and J/ψ decays contribute at higher momenta. Furthermore, there are sizable contributions from hadrons misidentified as electrons. To suppress low-multiplicity QED processes, including $\tau^+ \tau^-$ pairs, the number of charged tracks per event is required to be greater than three. This background and non-resonant hadronic events are further suppressed by a restriction on the ratio of Fox-Wolfram moments $H_2/H_0 < 0.4$ [10]. In semileptonic decays, the neutrino carries a substantial momentum. In events in which the only undetected particle is this neutrino, its direction can be inferred from the missing momentum in the event, defined as the difference between the net momentum of the two colliding beam particles and the vector sum of all detected particles, charged and neutral. Therefore, the selection of these decays can be greatly enhanced by requiring that the measured missing momentum exceed 1 GeV/ c and point into the detector fiducial volume. Furthermore, since the B mesons are produced almost at rest and the high momentum electron and neutrino point in nearly opposite directions, we require that the angle between the electron candidate and the missing momentum be greater than $\pi/2$. Candidate electrons are rejected if, when paired with an opposite-sign electron, the invariant mass of the pair is consistent with J/ψ mass, $3.05 < M_{e^+e^-} < 3.15$ GeV/ c^2 .

The detection efficiencies are estimated using Monte Carlo simulation. For the selection criteria described above, the detection efficiency for charmless semileptonic decays in the electron momentum interval of 1.5 – 2.7 GeV/ c ranges from ~ 0.4 to ~ 0.25 .

3.2 Background Subtraction

The raw spectrum of the highest momentum electron in events selected by the criteria described above is shown in Figure 1a, separately for data recorded ON and OFF resonance. For the OFF-resonance data, the momenta are scaled to compensate for the 0.4% difference in the c.m.s. energies of the two data samples.

Also shown in Figure 1a is a fit to approximate the non-resonant background contribution. For the purpose of this fit the normalized OFF-peak data in the interval of $p_{cms} = 1.5 - 3.5$ GeV/ c are combined with the ON-peak data in the interval of $p_{cms} = 2.7 - 3.5$ GeV/ c above the kinematic limit for $B \rightarrow X_u e \nu$ decays. The χ^2/dof for a fit with a 4-th degree Chebyshev polynomial is 51/51. Figure 1b shows the residuals of the fitted function from the unscaled OFF-peak data. The fit significantly reduces the statistical uncertainty in the estimate of the continuum background that is to be subtracted.

The result of the subtraction of the fitted continuum background is shown in Figure 2a. Also shown are the Monte Carlo predictions of the expected signal from $B \rightarrow X_u e \nu$ decays and background contributions from all other processes, $B \rightarrow X_c e \nu$. In this simulation, the $B \rightarrow X_u e \nu$ branching ratio is assumed to be $1 \cdot 10^{-3}$ and the relative normalization of data and Monte Carlo simulation is set by the number of electrons in the momentum interval between 1.5 and 2.3 GeV/ c . The result of the subtraction of all backgrounds is shown in Figure 2b.

The number of selected events, split into three momentum intervals, together with the estimated background contributions are listed in Table 1. The intervals are chosen to emphasize differences in the background composition: the interval 2.0 and 2.3 GeV/ c is dominated by semileptonic $B \rightarrow X_c e \nu$ decays, with a small contribution from hadron misidentification, the 2.3 – 2.6 GeV/ c interval is mostly populated by $B \rightarrow X_u e \nu$ decays and continuum background, while the 2.7 – 3.0 GeV/ c interval contains almost exclusively continuum background.

Table 1: The number of signal and background events and signal selection efficiencies $\epsilon(B \rightarrow X_u e \nu)$ for three different intervals in the electron momentum. N_{ON} refers to the number of selected electrons recorded on the $\Upsilon(4S)$ resonance, N_{OFF} is the fitted number of continuum background events. The $N(B \rightarrow X_c e \nu)$ and $N(B \rightarrow X_c \rightarrow e)$ refer to the Monte Carlo estimate of the remaining semileptonic background, from prompt and secondary decays (including $\psi(2S)$), respectively. $N(B \rightarrow J/\psi \rightarrow e^+ e^-)$ is an estimate of J/ψ background remaining after the mass cut. $N(B \rightarrow X_c)$ is a background from hadronic B decays to charm. $N(B \rightarrow X_u e \nu)$ is the resulting number of signal electrons.

Momentum p_e (GeV/ c)	2.0 – 2.3	2.3 – 2.6	2.7 – 3.0
N_{ON}	$74,140 \pm 272$	$6,455 \pm 80$	$1,932 \pm 44$
N_{OFF}	$7,749 \pm 165$	$4,051 \pm 93$	$1,903 \pm 37$
$N(B \rightarrow X_c e \nu)$	$61,158 \pm 470$	470 ± 41	0
$N(B \rightarrow J/\psi \rightarrow e^+ e^-)$	666 ± 49	128 ± 22	0
$N(B \rightarrow X_c \rightarrow e)$	338 ± 35	18 ± 8	0
$N(B \rightarrow X_c)$ - mis-ID	373 ± 37	92 ± 18	4 ± 4
$N(B \rightarrow X_u e \nu)$	$3,857 \pm 572$	$1,696 \pm 133$	25 ± 57
$\epsilon(B \rightarrow X_u e \nu)(\%)$	33.9 ± 1.0	27.7 ± 1.3	28.6 ± 22.9

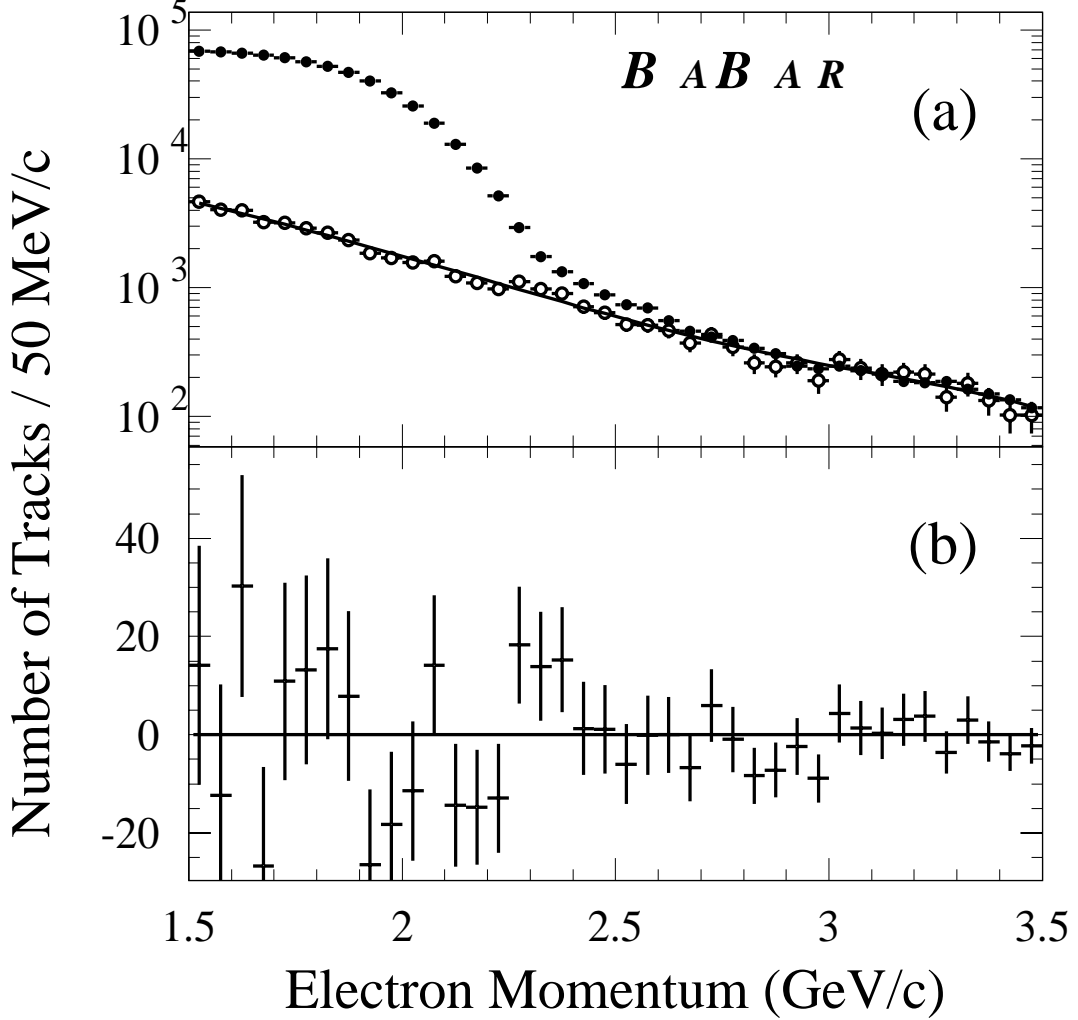


Figure 1: Electron momentum spectrum in the $\Upsilon(4S)$ rest frame: (a) ON-peak data (solid circles), OFF-peak data scaled by the ON/OFF-ratio (open circles), (b) OFF-peak data (unscaled) after the subtraction of the fitted continuum. The line show the result of a fit to the continuum spectrum (using both ON- and OFF-peak data) in the interval $p_{cms} = 1.5 - 3.5$ GeV/c with a 4-th degree Chebyshev polynomial.

3.3 Determination of $B \rightarrow X_u e \nu$ Branching Ratio

For a given interval in the electron momentum, the inclusive partial branching ratio is calculated according to

$$\Delta\mathcal{B} = \frac{N_{\text{ON}} - N_{\text{OFF}} - N_{B \rightarrow X_u e \nu}(1 + \delta_{\text{rad}})}{2\epsilon N_{B\bar{B}}}. \quad (1)$$

Here N_{ON} refers to the number of electrons detected ON-peak and N_{OFF} refers to the fitted contin-

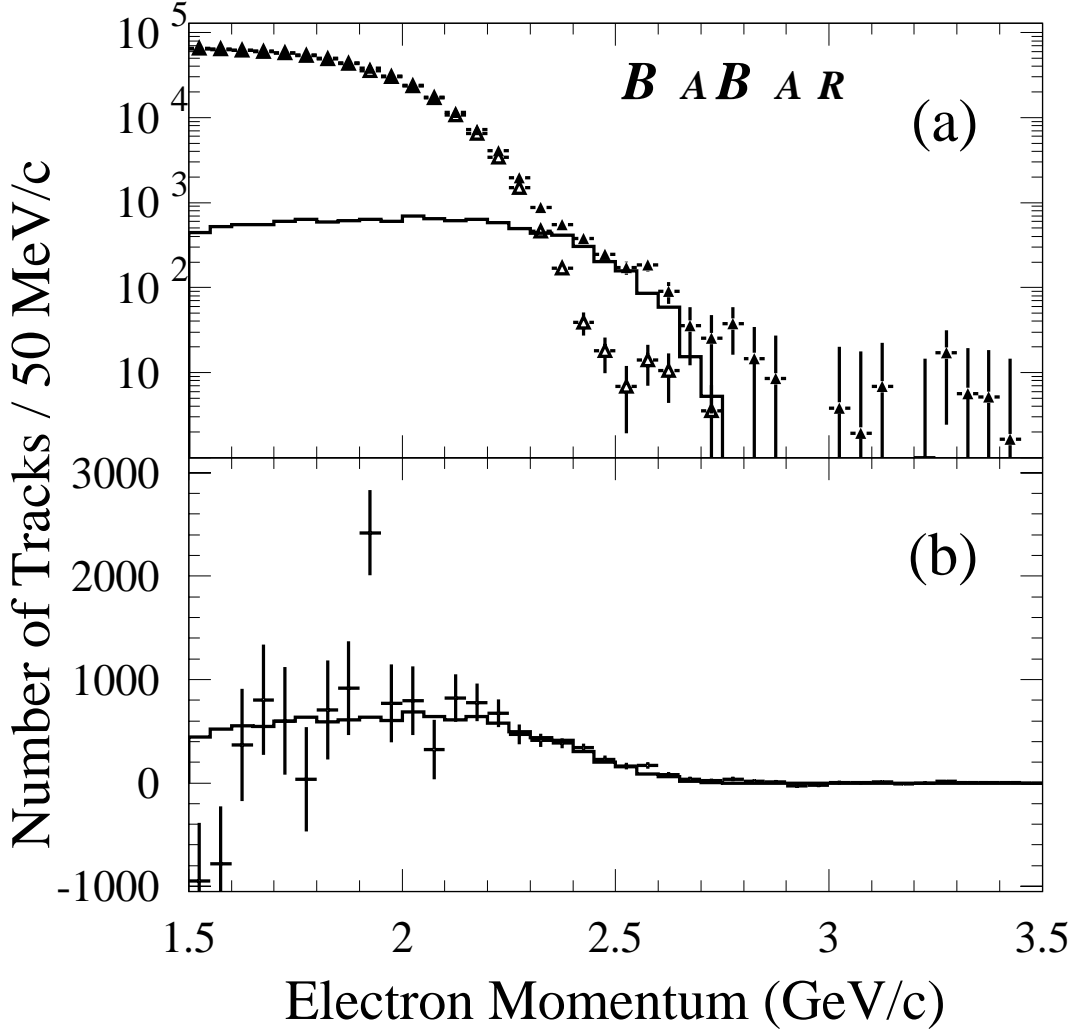


Figure 2: The electron momentum spectrum in the $\Upsilon(4S)$ rest frame: (a) ON-peak data after continuum subtraction (solid triangles), and MC predicted background from $B\bar{B}$ events ($B \rightarrow X_u e \nu$) (open triangles). (b) ON peak data after subtraction of continuum and Monte Carlo predicted ($B \rightarrow X_u e \nu$) backgrounds (data points with statistical errors). For comparison, the histograms show the expected signal spectrum from $B \rightarrow X_u e \nu$ decays.

uum background in a specified momentum interval, $N_{B \rightarrow X_u e \nu}$ is the background from $B\bar{B}$ events derived from Monte Carlo simulation normalized to the total number of electrons in the momentum range 1.5 – 2.3 GeV/c, ϵ is the total efficiency for detecting a signal electron from $B \rightarrow X_u e \nu$ decays (including bremsstrahlung in detector material), and δ_{rad} accounts for the distortion of the electron spectrum due to final-state radiation. This last is a momentum dependent correction, derived from the Monte Carlo simulation, amounting to $\sim 11\%$ in the range 2.3 – 2.6 GeV/c. As the overall normalization the total number of produced $B\bar{B}$ events is used, $N_{B\bar{B}} = (22,630 \pm 19 \pm 362) \cdot 10^3$.

The differential branching ratio as a function of the electron momentum in the $\Upsilon(4S)$ rest frame is shown in Figure 3. Integrated over the interval from 2.3 to 2.6 GeV/c, the partial branching ratio is (statistical error only):

$$\Delta\mathcal{B}(B \rightarrow X_u e \nu) = (0.152 \pm 0.014) \cdot 10^{-3}. \quad (2)$$

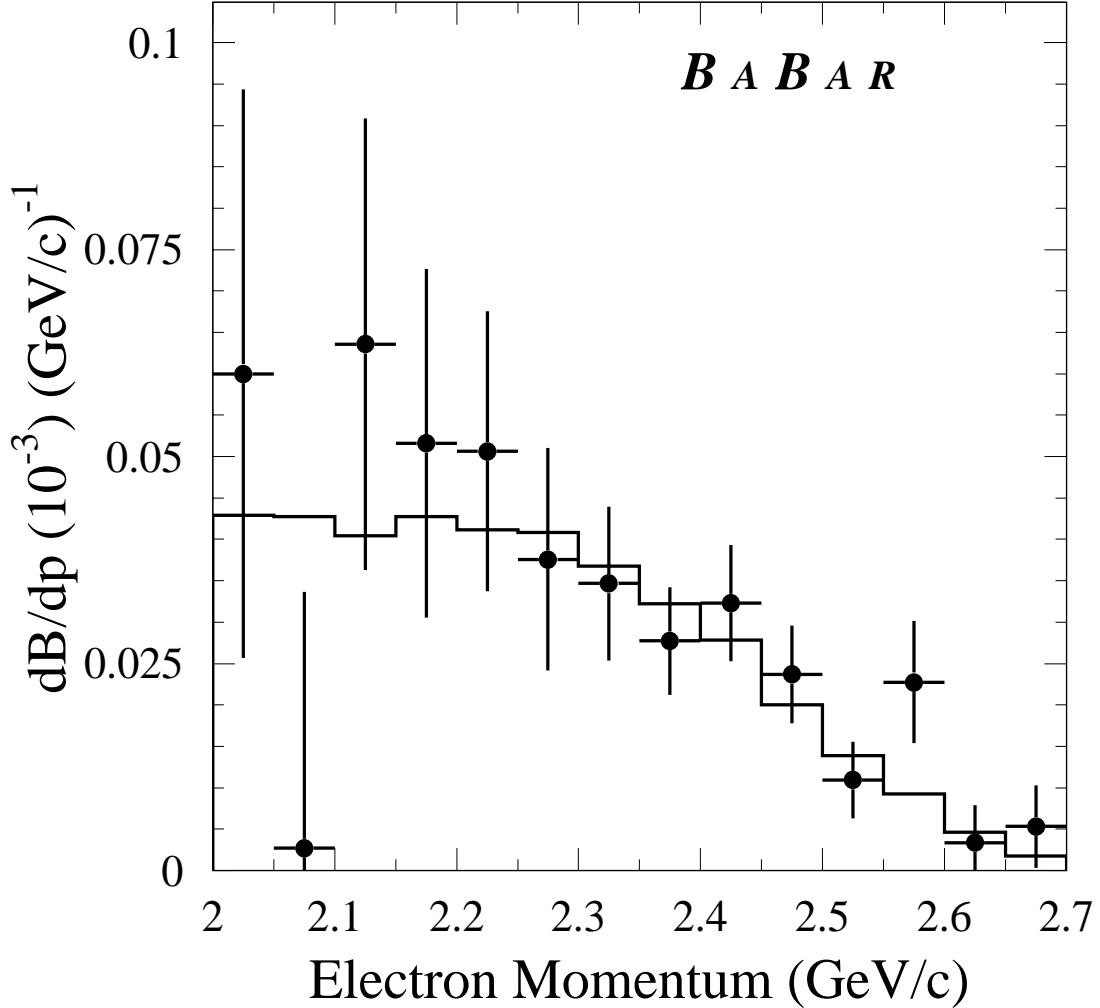


Figure 3: The branching ratio $\mathcal{B}(B \rightarrow X_u e \nu)$ as a function of the electron momentum in the $\Upsilon(4S)$ rest frame. The data (statistical errors only) are compared to a prediction (solid line) based on the ISGW2 model assuming a total inclusive branching ratio of $1 \cdot 10^{-3}$ for $B \rightarrow X_u e \nu$ decays with X_u masses up to $1.5 \text{ GeV}/c^2$. The spectrum is corrected for final-state radiation and bremsstrahlung.

3.4 Systematic Errors

The following sources of systematic errors have been considered:

- the Monte Carlo simulation of the signal events and the impact on the detection efficiency,
- continuum background subtraction,
- the subtraction of all other backgrounds based on Monte Carlo simulation of the production process and the detector simulation,
- the uncertainty of the B meson momentum spectrum in the $\Upsilon(4S)$ rest frame.

The systematic error introduced by the efficiency estimation for the signal events is caused by uncertainties in simulation of event selection (4%), the track reconstruction (1%), and the electron identification efficiencies (2%). The error on the selection efficiency depends not only on the accuracy of the detector model, but also on the adequacy of the ISGW2 model on which the event generation is based. The latter error has been estimated from the impact of the variation (within their current uncertainties) of individual branching ratios for B meson decays and variation of the event selection cuts. The total systematic error on the efficiency amounts to 5%.

An error in the continuum background subtraction can be introduced by the choice of the fitting function and the fitting procedure. The impact of the choice of the function has been estimated by trying different functional forms, such as an exponential function and Chebyshev polynomials. Possible differences in continuum spectra in ON-peak and OFF-peak data have been assessed by including or excluding ON-peak data above $B \rightarrow X_u e \nu$ kinematic limit in the fit. The observed variations in the number of continuum events leads us to attribute a 2% systematic uncertainty on the number of continuum events. This is equivalent to 5% systematic error in the number of signal events.

The $b \rightarrow c$ background consists of electrons and misidentified hadrons (see Table 1). The dominant contribution are electrons from semileptonic $B \rightarrow X_c e \nu$ decays. There is also a much smaller contribution of secondary electrons from $B \rightarrow X_c \rightarrow X_s e \nu$ and $B \rightarrow \psi(2S) \rightarrow ee$ decays, but very few with momenta above 2.3 GeV/ c . The error in the estimate of prompt lepton background arises primarily from the uncertainty in the decay dynamics and the branching fractions of the individual decay modes. The impact of these uncertainties (4%) is estimated by variation of these branching ratios within their current uncertainties. In addition, the uncertainty in the electron identification (2%) has been included. The systematic error (28%) on the background from misidentified hadrons arises from both the uncertainty in the spectrum of charged hadrons above 2.3 GeV/ c and the overall uncertainty on the mis-identification probabilities for pions and kaons. In addition, there is a small correction for electrons from J/ψ decays that are not vetoed by the mass requirement; the uncertainty in this correction is 20%. Background from photon conversions and Dalitz decays have been analyzed and found to be negligible above 1.5 GeV/ c . The total systematic error on the Monte Carlo based $b \rightarrow c$ background subtraction is estimated to be 6%, translating to a relative error of 3% on the number of signal events.

Since the $\Upsilon(4S)$ mass is so close to the threshold for $B\bar{B}$ production, the B meson momentum and thereby the endpoint of the electron spectrum from $B \rightarrow X_c e \nu$ decays is highly sensitive to the total energy of the colliding beams. Thus variations of the colliding beam energy introduces a systematic error in the $B \rightarrow X_c e \nu$ background subtraction. These variations are included in the Monte Carlo simulations, and the impact of the difference between data and Monte Carlo is studied using a sample of fully reconstructed B mesons. The comparison of the measured and simulated

momentum distributions, currently limited by statistics, shows that the systematic error from this effect does not exceed 5%.

In summary, Table 2 contains list of systematic errors for the momentum range from 2.3 to 2.6 GeV/ c ; the total systematic error on the partial branching ratio measurement for this momentum range is $\sim 9\%$.

Table 2: Systematic error on the $\Delta\mathcal{B}$ for the momentum range from 2.3 to 2.6 GeV/ c . All numbers are given in percent.

contribution	$\delta x/x$	$\delta(\Delta\mathcal{B})/\Delta\mathcal{B}$
efficiency $\epsilon(B \rightarrow X_u e \nu)$	5	5
continuum subtraction	2	5
background $B \rightarrow X_c e \nu$	4	1
background $B \rightarrow J/\psi \rightarrow e^+ e^-$	20	2
background $B \rightarrow X_c$ - mis-ID	28	2
B movement	5	5
$N_{B\bar{B}}$	1.6	1.6
radiative corrections	10	1
total	–	9

4 Conclusion

The result of this analysis, the fully corrected differential branching ratio as a function of the electron momentum in the $\Upsilon(4S)$ rest frame, is presented in Figure 3. Integrating over the interval from 2.3 to 2.6 GeV/ c results in the partial branching ratio

$$\Delta\mathcal{B}(B \rightarrow X_u e \nu) = (0.152 \pm 0.014 \pm 0.014) \cdot 10^{-3}. \quad (3)$$

This result agrees very well with the measurement by the CLEO collaboration [5]. The measured electron spectrum in the endpoint region is well reproduced by the ISGW2 model.

5 Extraction of $|V_{ub}|$ based on CLEO Measurements

To determine the charmless semileptonic branching fraction $\mathcal{B}(B \rightarrow X_u e \nu)$ from the partial branching fraction $\Delta\mathcal{B}(\Delta p)$, one needs to know the fraction $f_u(\Delta p)$ of the spectrum that falls into the momentum interval Δp . Heavy Quark theory describes the Fermi-motion of the quarks inside the meson in terms of a shape function that depends on non-perturbative QCD. To leading order, the same shape function describes all $b \rightarrow q\ell\nu$ transitions (here q represents any light quark).

The CLEO collaboration [11] has recently used the measurement of the inclusive photon spectrum from $b \rightarrow s\gamma$ transitions to derive the parameters describing the shape function and to calculate the lepton momentum spectrum for $B \rightarrow X_u e \nu$ transition. They quote a value of $f_u(\Delta p) = 0.074 \pm 0.014 \pm 0.009$ for the interval Δp from 2.3 to 2.6 GeV/ c .

Relying on the CLEO measurement, the result presented here translates into a total branching ratio of

$$\mathcal{B}(B \rightarrow X_u e \nu) = (2.05 \pm 0.27_{exp} \pm 0.46_{f_u}) \cdot 10^{-3}. \quad (4)$$

Based on studies developed independently by two groups [12]-[17], we adopt the following relationship for the extraction of $|V_{ub}|$ from the total branching fraction [18] (revised most recently at the 2002 CKM workshop)

$$|V_{ub}| = 0.00445 \left(\frac{\mathcal{B}(B \rightarrow X_u l \nu) 1.55 \text{ps}}{0.002 \tau_b} \right)^{1/2} (1.0 \pm 0.020 \pm 0.052), \quad (5)$$

where the first error arises from the uncertainty in the OPE expansion, and the second from the uncertainty in the b quark mass, assuming $m_b(1 \text{ GeV}) = 4.58 \pm 0.09 \text{ GeV}$. Based on this expression and our measurement of the branching fraction, we find

$$|V_{ub}| = (4.43 \pm 0.29_{exp} \pm 0.25_{OPE} \pm 0.50_{f_u} \pm 0.35_{s\gamma}) \cdot 10^{-3}. \quad (6)$$

Here the first error is the measurement uncertainty from the combined statistical and systematic error, and the second refers to the uncertainty on the extraction of $|V_{ub}|$ from the branching ratio as stated above. The remaining errors are taken from the CLEO analysis: the third refers to the determination of f_u and the fourth represents an estimate of the validity of the assumption that the shape function can be extracted from the $b \rightarrow s\gamma$ spectrum. The uncertainty due to the theoretical assumption of quark-hadron duality remains unquantifiable.

The *BABAR* collaboration is planning to develop this and other methods for extracting the total branching ratio and $|V_{ub}|$ in the near future.

6 Acknowledgments

We are grateful for the extraordinary contributions of our PEP-II colleagues in achieving the excellent luminosity and machine conditions that have made this work possible. The success of this project also relies critically on the expertise and dedication of the computing organizations that support *BABAR*. The collaborating institutions wish to thank SLAC for its support and the kind hospitality extended to them. This work is supported by the US Department of Energy and National Science Foundation, the Natural Sciences and Engineering Research Council (Canada), Institute of High Energy Physics (China), the Commissariat à l’Energie Atomique and Institut National de Physique Nucléaire et de Physique des Particules (France), the Bundesministerium für Bildung und Forschung and Deutsche Forschungsgemeinschaft (Germany), the Istituto Nazionale di Fisica Nucleare (Italy), the Research Council of Norway, the Ministry of Science and Technology of the Russian Federation, and the Particle Physics and Astronomy Research Council (United Kingdom). Individuals have received support from the A. P. Sloan Foundation, the Research Corporation, and the Alexander von Humboldt Foundation.

References

- [1] J. Chay, H. Georgi, and B. Grinstein, Phys. Lett. **B247**, 399 (1990).
- [2] The ARGUS Collaboration, H. Albrecht *et al.*, Phys. Lett. **B234**, 409 (1990).
- [3] The ARGUS Collaboration, H. Albrecht *et al.*, Phys. Lett. **B255**, 297 (1991).
- [4] The CLEO Collaboration, R. Fulton *et al.*, Phys. Rev. Lett. **64**, 16 (1990).

- [5] The CLEO Collaboration, F. Bartelt *et al.*, Phys. Rev. Lett. **71**, 4111 (1993).
- [6] The BABAR Collaboration, B. Aubert *et al.*, Nucl. Instrum. Methods. **A479**, 1 (2002).
- [7] N. Isgur, D. Scora, B. Grinstein, and M.B. Wise, Phys. Rev. **D39**, 799 (1989); D. Scora, N. Isgur, Phys. Rev. **D52**, 2783 (1995).
- [8] I.I. Bigi, M. Shifman, and N.G. Uraltsev, Annu. Rev. Nucl. Part. Sci. **47**, 591 (1997).
- [9] J.L. Goity and W. Roberts, Phys. Rev. **D51**, 3459 (1995).
- [10] G.C. Fox and S. Wolfram, Phys. Rev. Lett. **41**, 1581 (1978).
- [11] The CLEO Collaboration, A. Bornheim *et al.*, hep-ex/0202019 (2002).
- [12] N. Uraltsev, Int. J. Mod. Phys. **A11**, 515 (1996).
- [13] I.I. Bigi, M. Shifman, and N. Uraltsev, TPI-MINN-97/02-T, UMN-TH-1528-97, UND-HEP-97-BIG01, hep-ph/9703290 (1997).
- [14] N. Uraltsev, Int. J. Mod. Phys. **A14**, 4641 (1999).
- [15] I.I. Bigi, UMN-HEP-BIG-99-05, hep-ph/9907270 (1999).
- [16] A.H. Hoang, Z. Ligeti, and A.V. Manohar, Phys. Rev. Lett. **82**, 277 (1999).
- [17] A.H. Hoang, Z. Ligeti, and A.V. Manohar, Phys. Rev. **D59**, 074017 (1999).
- [18] Combined results on b-hadron production rates and decay properties, CERN-EP/2001-050 (2001).